a- and *c*-axis resistivity and magnetoresistance in $MoCl_5$ graphite intercalation compounds

1999 J. Phys.: Condens. Matter 11 3149

(http://iopscience.iop.org/0953-8984/11/15/020)

J. Phys.: Condens. Matter **11** (1999) 3149–3160. Printed in the UK PII: S0953-8984(99)95263-3

a- and c-axis resistivity and magnetoresistance in $MoCl_5$ graphite intercalation compounds

Keiko Matsubara†‖, Ko Sugihara‡, Itsuko S Suzuki§ and Masatsugu Suzuki§

† Department of Electrical Engineering, College of Science and Technology, Nihon University, Chiyoda-ku, Tokyo 101, Japan
‡ College of Pharmacy, Nihon University, Funabashi, Chiba 274, Japan
§ Department of Physics, State University of New York at Binghamton, Binghamton, NY 13902-6016, USA

Received 19 June 1998, in final form 1 December 1998

Abstract. The a-axis electrical resistivity ρ_a and the transverse magnetoresistance (aT-MR ($\boldsymbol{H} \parallel \boldsymbol{c}$)) of stage-2 to 6 $MoCl_5$ graphite intercalation compounds (GICs) have been measured in the temperature (T) range between 4.2 and 300 K and magnetic field (H) range between 0 and 7 kOe. The data are analysed together with the results of c-axis resistivity ρ_c and the longitudinal magnetoresistance (cL-MR ($\boldsymbol{H} \parallel \boldsymbol{c}$)) reported in our previous work. For stage-2 to 5 $MoCl_5$ GICs ρ_a shows a metallic-like T dependence and exhibits no logarithmic behaviour, while ρ_c shows a metallic-like behaviour for low stage (2), a logarithmic behaviour for the intermediate stages (3, 4) and a semiconductor-like behaviour for high stages (5, 6). For all stages the sign of aT-MR ($\boldsymbol{H} \parallel \boldsymbol{c}$) is positive, while the sign of cL-MR ($\boldsymbol{H} \parallel \boldsymbol{c}$) is negative for the intermediate stages (3–5) and positive for low stages in low T and weak H. The resistivity ρ_c is formed of a series connection of G–I–G (G: graphite layer, I: intercalate layer) and G–G resistivity, while ρ_a is formed of a parallel connection of each layer contribution. The behaviour difference between ρ_a and ρ_c is discussed in the light of the role of the interior G layer forming a bottleneck to the c-axis conduction. The logarithmic behaviour and negative magnetoresistance in ρ_c arise from the two-dimensional weak localization occurring in these interior G layers.

1. Introduction

In the past two decades c-axis electrical resistivity measurements have been carried out for various kinds of graphite intercalation compound (GIC) with a staging structure along the c-axis [1–12]. For stage-n GICs there are n graphite (G) layers between adjacent intercalate (I) layers. Models on the c-axis conduction mechanism have been proposed to explain these results [13–17]. The overlapping of a wave function of carrier over adjacent G layers in GICs is crucial to the c-axis conduction. Depending on the degree of the overlapping the following two models are proposed: a two-dimensional (2D) band model and a three-dimensional (3D) band model. In a 2D band model there is no overlapping of the wave function over nearest neighbour G layers: carriers are localized in each G layer. Since the I layers are electrically insulating in acceptor GICs, this model may be appropriate at least for low stages. In this model the c-axis conduction can occur through a hopping of carriers between G layers through a conduction-channel (conduction-path) Hamiltonian. However, this 2D conduction model may not be true for pristine graphite and donor GICs because of relatively strong correlation

‖ Present address: Energy Laboratory, Electronic Research Centre, Samsung Yokohama Research Institute, 2–7, Sugasawa-cho, Tsurumi-ku, Yokohama 230-0027, Japan.

0953-8984/99/153149+12$19.50

between G layers. The I layers are usually electrically conductive in donor GICs. The wave function of carriers is not localized in each G layer (a 3D band model), leading to the bandlike conduction along the c-axis. Even for acceptor GICs it may be reasonable to assume that the character of the conduction band changes from 2D- to 3D-like for high stages.

In a previous paper [11] we have reported the temperature (T) dependence of the c-axis resistivity (ρ_c) and longitudinal magnetoresistance ($\Delta\rho_{cT}/\rho 0$, cL-MR ($\boldsymbol{H} \parallel \boldsymbol{c}$)) of stage-2 to 6 $MoCl_5$ GICs, where $\boldsymbol{H}$ is an external magnetic field. We have found (i) a metallic behaviour in stage 2, (ii) a logarithmic behaviour at low T in stage 3 and 4 and a negative magnetoresistance (n-MR) at low T and weak H in stage 3 to 5 and (iii) a semiconductor-like behaviour in high stages (5, 6). We have shown that these results can be qualitatively explained within the framework of a 2D band model with a hopping conduction mechanism. Carriers diffuse along each G layer and occasionally make transitions to the nearest neighbour G layers through hopping. The logarithmic behaviour and negative magnetoresistance are due to a 2D weak localization effect (WLE) occurring in the interior G layer in high-stage $MoCl_5$ GICs.

In most of the studies on electrical resistivity in GICs so far, measurements were restricted to one direction (a- or c-axis) and little attention has been paid to the correlation between a- and c-axis conduction and systematic study of their stage dependence. As far as we know, there are few detailed attempts [18] to compare the experimental results of ρ_a with those of ρ_c for the same sample, partly because of the problem of their stability or resolution. On this point, $MoCl_5$ GICs are suitable for investigation, because they are stable under ambient atmosphere and the reproducibility of the resistivity is good when repeating the examination with decreasing or increasing T.

In the present work we report experimental results of the a-axis resistivity (ρ_a) and a-axis transverse magnetoresistance ($\Delta\rho_{aT}/\rho_0$, aT-MR ($\boldsymbol{H} \parallel \boldsymbol{c}$)) for stage-2 to 6 $MoCl_5$ GICs. We also examine the c-axis transverse magnetoresistance ($\Delta\rho_{cT}/\rho_0$, cT-MR ($\boldsymbol{H} \parallel \boldsymbol{a}$)) in association with the negative component of cL-MR ($\boldsymbol{H} \parallel \boldsymbol{c}$). The samples used in the present work are the same as those used in the previous work [11]. We will show that for stage-2 to 5 $MoCl_5$ GICs ρ_a shows a metallic T dependence and exhibits no logarithmic behaviour, while the sign of aT-MR ($\boldsymbol{H} \parallel \boldsymbol{c}$) is positive for all stages. These results seem to be rather different from those obtained from ρ_c and cL-MR ($\boldsymbol{H} \parallel \boldsymbol{c}$). We will show that such a difference can be qualitatively explained within the framework of the 2D band model with a hopping conduction mechanism.

2. 2D band model with hopping conduction: c- and a-axis resistivity

Here we present a simple model for the c-axis and a-axis resistivity of acceptor GICs which has been proposed by Sugihara *et al* [13, 15–17], assuming that hopping conduction occurs between G layers having 2D bands. The carriers diffuse along each G layer for a sufficiently long time and occasionally transfer to the neighbouring G layers with the aid of a conduction-channel (conduction path) Hamiltonian. Thus the c-axis conductivity of the regions G–G and G–I–G is determined mainly by the in-plane conductivity of the related G layers. There are two kinds of G layer for high stage GICs ($n \geqslant 3$). Due to the attractive Coulomb interaction between I and G layers, the transfer charge density is mostly concentrated on the bounding G layers (G_b), while a small amount of charge density is distributed on the interior G layers (G_i). The in-plane conductivity along the G_b layer may be much larger than along the G_i layer.

The c-axis conductivity $\sigma_c(G_bIG_b)$ for the G_bIG_b sandwich is approximated as $(m_b\bar{h}/\Gamma_b)|H(G_bIG_b)|^2$, where m_b is an effective mass of carriers in G_b layers, $\Gamma_b/\bar{h}$ is the in-plane scattering rate and $H(G_bIG_b)$ is the interlayer transition matrix element of the conduction-channel Hamiltonian. The c-axis conductivity between the adjacent G_b layers

$(= \sigma_c(G_bG_b))$, which appears only for $n = 2$, is approximated by $(m_b\overline{h}/\Gamma_b)|H(G_bG_b)|^2$. The c-axis conductivity between the G_b layer and G_i layer $(= \sigma_c(G_bG_i))$, which appears for $n \geqslant 3$, is approximated by $(m_b\overline{h}/\Gamma_b + m_i\overline{h}/\Gamma_i)|H(G_bG_i)|^2/2$, where m_i is the effective mass of carriers in G_i layers and $\Gamma_i/\overline{h}$ is the in-plane scattering rate. The c-axis conductivity between the adjacent G_i layers $(= \sigma_c(G_iG_{i+1}))$, which appears for $n \geqslant 4$, is approximated by $(m_i\overline{h}/\Gamma_i + m_{i+1}\overline{h}/\Gamma_{i+1})|H(G_iG_{i+1})|^2/2$.

The resultant c-axis resistivity of stage-n GICs, ρ_c, consists of the following resistivities in series: $\rho_c(G_bIG_b) = [\sigma_c(G_bIG_b)]^{-1}$, $\rho_c(G_bG_b) = [\sigma_c(G_bG_b)]^{-1}$, $\rho_c(G_bG_i) = [\sigma_c(G_bG_i)]^{-1}$ and $\rho_c(G_iG_{i+1}) = [\sigma_c(G_iG_{i+1})]^{-1}$. For stage-1 GIC ρ_c is equal to $\rho_c(G_bIG_b)$. For stage-2 GIC with $G_bIG_bG_bI\ldots$ as a c-axis stacking sequence, ρ_c is expressed by

$$\rho_c = \frac{1}{I_c^{(2)}}[d_I\rho_c(G_bIG_b) + d_G\rho_c(G_bG_b)] \tag{1}$$

where $I_c^{(n)}$ denotes the c-axis repeat distance of stage-n GIC and d_I and d_G are the distances between nearest neighbour G layers with and without an intervening I layer, respectively. For stage-5 GIC with $G_bIG_bG_1G_2G_1G_bI\ldots$ as a c-axis stacking sequence, for example ρ_c is expressed by

$$\rho_c = \frac{1}{I_c^{(5)}}[d_I\rho_c(G_bIG_b) + 2d_G\rho_c(G_bG_1) + 2d_G\rho_c(G_1G_2)]. \tag{2}$$

In contrast, the in-plane conductivity of stage-n GIC, σ_a, is approximated by a sum of the in-plane conductivity of each G layer because of parallel connection of the in-plane resistivity contribution of G layers. The in-plane conductivity $\sigma_a(G_b)$ for the G_b layer and $\sigma_a(G_i)$ for the G_i layer are described as $\sigma_a(G_b) = n_be^2\tau_b/m_b$ and $\sigma_a(G_i) = n_ie^2\tau_i/m_i$, respectively, where τ_b and τ_i are the in-plane relaxation times of carriers, and n_b and n_i are the carrier concentrations in the G_b and G_i layers, respectively. For example, σ_a is equal to $\sigma_a(G_b)$ for stage-2 GIC and is approximated by

$$\sigma_a = \tfrac{1}{5}[2\sigma_a(G_b) + 2\sigma_a(G_1) + \sigma_a(G_2)] \tag{3}$$

for stage-5 GIC. Note that the relaxation rate $1/\tau$ is related to $\Gamma/\overline{h}$ by

$$\frac{1}{\tau} = \int \mathrm{d}\theta(1-\cos\theta)\frac{\Gamma}{\overline{h}} \tag{4}$$

where θ is an angle between the incoming and outgoing wave vectors of carriers. Except at low T where the forward (small angle) scattering factor $(1-\cos\theta)$ is important, τ is assumed to be equal to $\overline{h}/\Gamma$: $\tau_b \approx \overline{h}/\Gamma_b$ and $\tau_i \approx \overline{h}/\Gamma_i$.

Now we add the following assumption to the above model: a 2D WLE occurs only in the interior G layers. The weak localization of carriers arises from the interference between the electron waves, which are related to each other through a time reversal scattering process. The in-plane relaxation rate of interior G layers (Γ_i) is assumed to be much larger than that of bounding G layers (Γ_b). Then the c-axis resistivity is dominated by $\rho_c(G_iG_{i+1})$ for interior G layers, forming a bottleneck to the c-axis conduction. In contrast, the a-axis resistivity is dominated by the in-plane resistivity $[\sigma_a(G_b)]^{-1}$ for bounding G layers. Thus a logarithmic behaviour which is one of the characteristics of the 2D WLE is predicted to appear in ρ_c. The interference effect can be partly destroyed by the application of H, inducing a negative magnetoresistance (N-MR) component. Since the orbital motion of carriers in interior G layers is influenced by the application of H parallel to the c-axis, an N-MR is predicted to appear only in the longitudinal c-axis magnetoresistance.

3. Experimental procedure

Host graphite used in the present work was highly oriented pyrolytic graphite (HOPG). $MoCl_5$ GIC samples were prepared by heating a mixture of HOPG and powdered $MoCl_5$ in a two-zone furnace. The staging structure was determined by x-ray diffraction [11]. Samples had a rectangular form with typically a base of 6 mm $\times$ 4 mm and a height of 0.4 mm along the c-axis. The measurements of a-axis resistivity ρ_a were made using a conventional four-probe method. Two pairs of gold wires as the current and voltage probes were attached to samples by silver paste (4922N, du Pont). The current (10 mA) was supplied through the current probes by a Yokogawa 7651 programmable DC current source. The voltage generated across the voltage probes was measured by a Keithley 181 nanovoltmeter. Magnetoresistance was measured in the presence of H changing stepwise 0 to 7 kOe at T between 4.2 and 300 K.

4. Results and discussion

4.1. T-dependence of a- and c-axis resistivity

In the previous paper [11], we reported the T dependence of ρ_c for stage-2 to 6 $MoCl_5$ GICs. The resistivity ρ_c for stage-2 $MoCl_5$ GIC exhibits a metallic-like T dependence for $4.2 \leqslant T \leqslant 300\ K$, while ρ_c for stage 3 and 4 shows a logarithmic behaviour below 20 K and monotonically increases with increasing T above 20 K. For stage 5 ρ_c has a local minimum around 40 K and a maximum at 128 K, and shows a relatively abrupt decrease above 128 K. The T dependence of ρ_c for stage 6 also has a local minimum at 184 K and increases with further increasing T. The T dependence of ρ_c changes continuously from metallic-like to semiconductor-like with increasing stage number n.

In figure 1 we show the T dependence of ρ_a for stage-2 to 6 $MoCl_5$ GICs. The features of figure 1 are summarized as follows. (i) The value of ρ_a at 4.2 K simply increases with increasing n except for stage 2. (ii) The value of ρ_a for stage 3 to 5 is smaller than that of the host material HOPG. (iii) ρ_a shows a metallic-like behaviour for all stages. Note that no logarithmic behaviour is observed at any T. (iv) The derivative $\mathrm{d}\rho_a/\mathrm{d}T$ is almost the same except for stage 2.

In figure 2 we show the T dependence of normalized resistivity defined by ξ_p $(= (\rho_p(T) - \rho_p(4.2\ K))/(\rho_p(295\ K) - \rho_p(4.2\ K)))$ with $p = a$ and c for stage-2 $MoCl_5$ GIC. We find that the T dependence of ξ_c is in good agreement with that of ξ_a at least below 150 K. This result may be explained as follows. In the model described in section 2, the c-axis resistivity ρ_c for stage 2 is predicted to be proportional to $(\Gamma_b/\overline{h})\{|H(\mathrm{G}_b\mathrm{G}_b)|^{-2} + |H(\mathrm{G}_b\mathrm{I}\mathrm{G}_b)|^{-2}\}$, while the in-plane resistivity ρ_a is described by $m_b/(n_b e^2 \tau_b)$, where $1/\tau_b$ is related to $\Gamma_b/\overline{h}$ by (4). If $1/\tau_b \approx \Gamma_b/\overline{h}$, and $|H(\mathrm{G}_b\mathrm{G}_b)|^{-2}$ and $|H(\mathrm{G}_b\mathrm{I}\mathrm{G}_b)|^{-2}$ are independent of T, both ρ_c and ρ_a are proportional to $\Gamma_b/\overline{h}$, leading to the relation $\xi_c = \xi_a$. It may be concluded that the conduction mechanism of ρ_c and ρ_a is controlled by the in-plane relaxation rate Γ_b. The slight deviation of ξ_c from ξ_a may suggest that (i) $\Gamma_b/\overline{h}$ is not strictly equal to τ_b, and that (ii) the interlayer matrix element is assumed to be weakly dependent on T.

In the case of $n \geqslant 4$, the T dependence of ρ_c is modified by the contribution of $\rho_c(\mathrm{G}_i\mathrm{G}_{i+1})$, where G_i and G_{i+1} are interior G layers. Note that $\rho_c(\mathrm{G}_i\mathrm{G}_{i+1})$ is completely different from the resistivity of pure graphite derived from the 3D band model. The c-axis resistivity $\rho_c(\mathrm{G}_i\mathrm{G}_{i+1})$ is proportional to $(\Gamma_i/\overline{h})|H(\mathrm{G}_i\mathrm{G}_{i+1})|^{-2}$, where $|H(\mathrm{G}_i\mathrm{G}_{i+1})|^2$ is a sum of the elastic scattering contribution $|H(\mathrm{G}_i\mathrm{G}_{i+1})^{(i)}|^2$ due to impurities or defects and the inelastic scattering contribution $|H(\mathrm{G}_i\mathrm{G}_{i+1})^{(e-p)}|^2$ due to out-of-plane mode phonons. The T dependence of $|H(\mathrm{G}_i\mathrm{G}_{i+1})|^2$ comes from that of $|H(\mathrm{G}_i\mathrm{G}_{i+1})^{(e-p)}|^2$, which increases with increasing T.

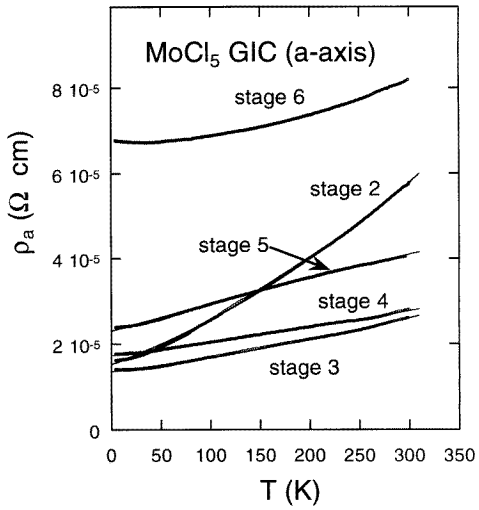

Figure 1. T dependence of ρ_a for stage-2 to 6 $MoCl_5$ GICs. Solid lines are results of the curve fitting based on (5).

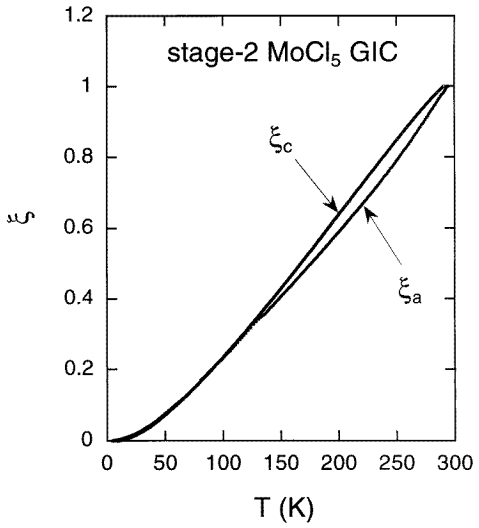

Figure 2. Normalized a- and c-axis resistivity ξ_p $(= (\rho_p(T) - \rho_p(4.2\ K))/(\rho_p(295\ K) - \rho_p(4.2\ K)))$ against T for stage-2 $MoCl_5$ GIC with $p = a$ and c.

Since $\Gamma_i/\overline{h}$ increases with T and $|H(G_iG_{i+1})|^{-2}$ decreases with T, the T dependence of $\rho_c(G_iG_{i+1})$ results from the competition between these two factors. With increasing n the contribution from $|H_{GG}^{(e-p)}|^2$ becomes dominant compared to that of $\Gamma_i/\overline{h}$, leading to the change of T dependence of ρ_c from metallic-like to semiconductor-like. Consequently the T dependence of ρ_c gradually differs from that of ρ_a with increasing n.

No logarithmic behaviour is observed in ρ_a for all stages, while a logarithmic behaviour is observed in ρ_c for intermediate stages (3, 4). These results suggest that the 2D WLE occurs in the interior G layers. The c-axis resistivity ρ_c is formed of series connection of resistivities

$\rho_c(G_bIG_b)$, $\rho_c(G_bG_1)$, $\rho_c(G_1G_2)$, ... along the c-axis. The interior G layers form a bottleneck to the c-axis conduction. The T dependence of ρ_c mainly comes from that of the bottleneck resistivity. In contrast, the a-axis resistivity is formed of parallel connection of the in-plane resistivity contribution of each G layer. When the in-plane conductivity of bounding G layers is much larger than that of interior G layers, the T dependence of ρ_a mainly comes from that of the in-plane relaxation rate $\Gamma_b/\hbar(=1/\tau_b)$ of bounding G layers.

Here we discuss the T dependence of ρ_a for $MoCl_5$ GICs. It is generally accepted that the T dependence of ρ_a for many kinds of acceptor type GIC can be described as

$$\rho_a(T) = A + BT + CT^2 \tag{5}$$

where A, B and C are constants [19]. Here the BT term is due to the intrapocket electron phonon scattering which is dominant in the intermediate T ranges, while the CT^2 term is due to the interpocket scattering process suggested by Kamimura *et al* [19]. For stage-2 to 5 $MoCl_5$ GICs the least squares fit of our data (ρ_a against T) to (5) yields parameters A, B and C as listed in table 1 (ρ_a for stage 6 is not included because of its local minimum). For stage 2, the contribution of the T^2 term is more important than that of stage 3 to 5, suggesting that the larger the Fermi surface, the stronger the interpocket scattering. The GICs with $n \geqslant 3$ have several bands and the corresponding Fermi surfaces. The interpocket scattering associated with interior G layers is weaker than that with bounding G layers. However, so far we have no reasonable explanation for the interpocket scattering which is more effective for the low-stage GICs. Here we show an alternative model which may explain the dominant contribution of the T^2 term for low stages. The phonon wave vector $\boldsymbol{q}_a$ contributing to the intrapocket scattering mediated by the in-plane phonon has a limited value of $0 < q_a < 2k_F$, where k_F is the Fermi wave number. A typical value of k_F for low stages is $\sim 10^7$ cm^{-1}, and thus the maximum phonon energy is of the order of $2\hbar v_s k_F/k_B = 320\ K$ where $k_F = 10^7$ cm^{-1} and sound velocity $v_s = 2.1 \times 10^6$ cm s^{-1}, implying that the phonon distribution cannot be treated as the classical one. The deviation of ρ_a from T-linear dependence is predicted to appear below 300 K. This is the reason why $d\rho_a/dT$ for stage 2 is larger than that for stage 3 to 6. The features of the data given by table 1 can be qualitatively explained by the above model. As most of the charge transfer occurs between bounding G layers, however, the T^2 term remains even for high stages. Therefore the T dependence of ρ_a still shows a metallic-like behaviour for high stages.

Table 1. Parameters obtained from least squares fitting of data (ρ_a) to (5) for stage-2 to 5 $MoCl_5$ GICs, where n is the stage number.

n	A ($\times 10^{-5}$ Ω cm)	B ($\times 10^{-8}$ Ω cm K^{-1})	C ($\times 10^{-10}$ Ω cm K^{-2})
2	1.525	8.477	1.915
3	1.362	2.781	0.457
4	1.736	2.877	0.193
5	2.307	6.441	−0.161

4.2. Magnetoresistance

4.2.1. c-axis transverse magnetoresistance. In the previous paper [11] we have studied the T and H dependence of the c-axis longitudinal magnetoresistance $\Delta\rho_{cL}/\rho_0$ (cL-MR ($\boldsymbol{H} \parallel \boldsymbol{c}$)) for stage-2 to 6 $MoCl_5$ GICs. The N-MR of ρ_c is observed at low H and low T for the intermediate stages (3–5). This result has been discussed in terms of the 2D WLE which occurs in the interior

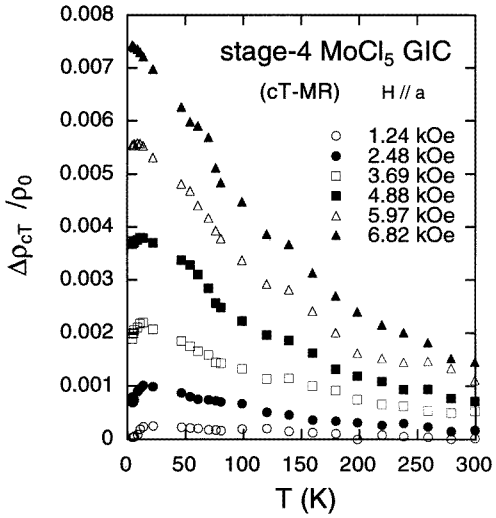

Figure 3. T dependence of c-axis transverse magnetoresistance (cT-MR, $\boldsymbol{H} \parallel \boldsymbol{a}, \boldsymbol{E} \parallel \boldsymbol{c}$) for stage-4 $MoCl_5$ GIC, where $\boldsymbol{E}$ is an electric field.

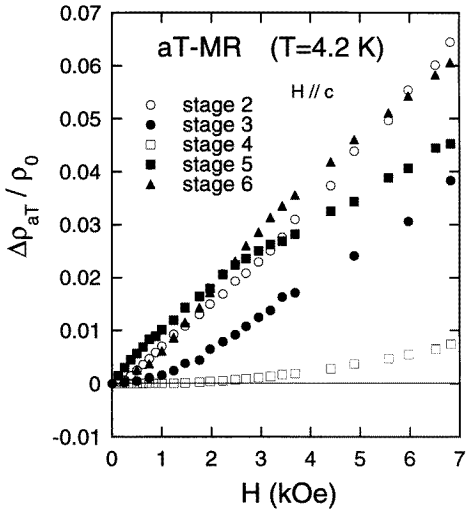

Figure 4. H dependence of $\Delta\rho_{aT}/\rho_0$(aT-MR, $\boldsymbol{H} \parallel \boldsymbol{c}$, $\boldsymbol{E} \parallel \boldsymbol{a}$) at 4.2 K for stage-2 to 6 $MoCl_5$ GICs.

G layers. The appearance of N-MR is closely related to a partial destruction of the interference effect by the application of H along the c-axis.

What happens to ρ_c when H is applied along the c-plane? Can the N-MR be still observed for stage-3 to 5 $MoCl_5$ GICs? Figure 3 shows the T dependence of $\Delta\rho_{cT}/\rho_0$ (cT-MR ($\boldsymbol{H} \parallel \boldsymbol{a}$)) for field $H = 1.24$, 2.48, 3.69, 4.88, 5.97 and 6.82 kOe. We find that the sign of cT-MR ($\boldsymbol{H} \parallel \boldsymbol{a}$) is positive all over the T and H ranges in contrast to the negative sign of cL-MR ($\boldsymbol{H} \parallel \boldsymbol{c}$) shown in figure 8 of [11]. The peak around 20 K indicates that a component of N-MR slightly exists below 20 K, although the sign of the observed cT-MR ($\boldsymbol{H} \parallel \boldsymbol{a}$) is still positive. The difference between cT-MR ($\boldsymbol{H} \parallel \boldsymbol{a}$) and cL-MR ($\boldsymbol{H} \parallel \boldsymbol{c}$) indicates that the 2D WLE is strongly dependent on the direction of H. The orbital motion of carriers in the interior G layers

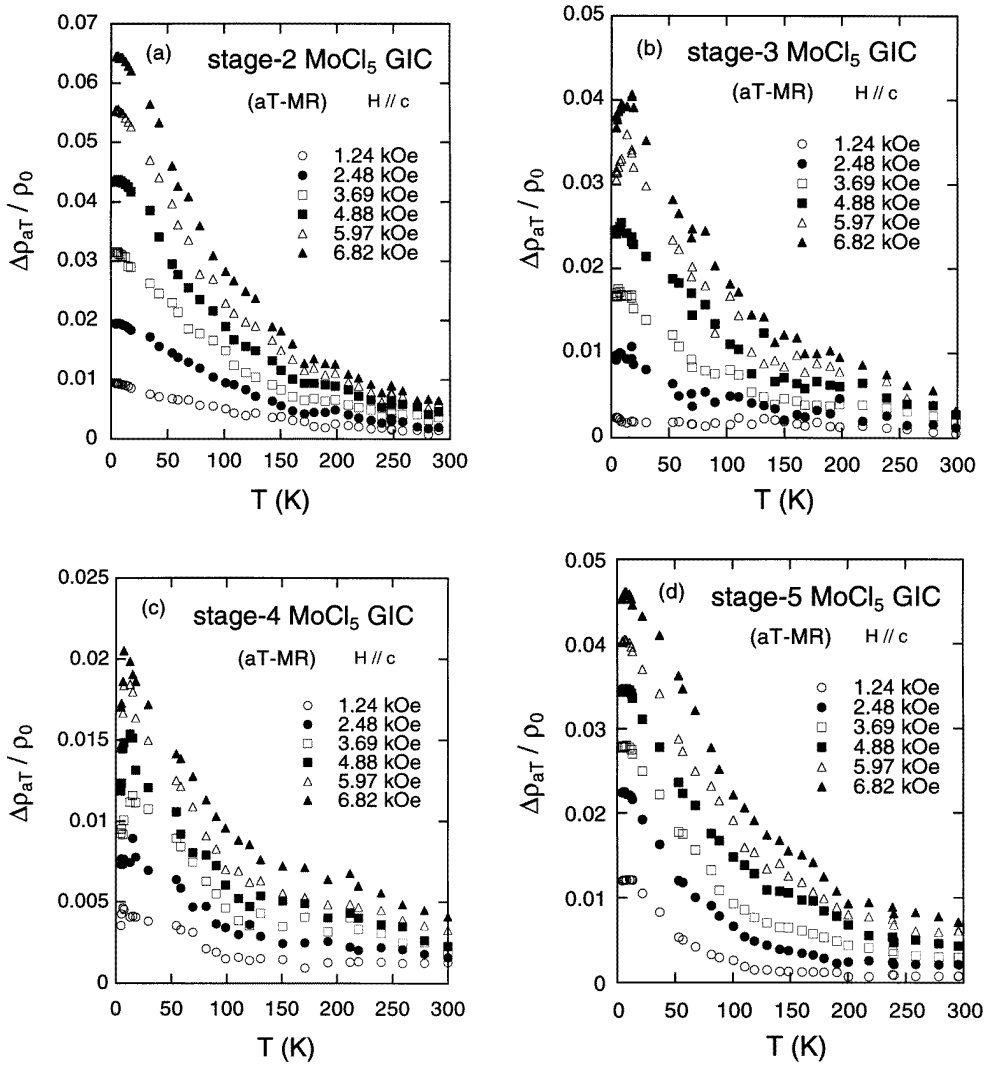

Figure 5. T dependence of a-axis transverse magnetoresistance (aT-MR, $\boldsymbol{H} \parallel \boldsymbol{c}$, $\boldsymbol{E} \parallel \boldsymbol{a}$) for (a) stage-2, (b) 3, (c) 4, (d) 5 and (e) 6 $MoCl_5$ GICs. $H = 1.24$, 2.48, 3.69, 4.88, 5.97 and 6.82 kOe.

is influenced only by the application of H along the c-axis. This behaviour is not due to the Zeeman effect for electron spins which does not strongly depend on the direction of H.

In the previous paper [11] we discussed the possibility of the Kondo effect as a cause for the logarithmic behaviour of ρ_c and N-MR of cL-MR ($\boldsymbol{H} \parallel \boldsymbol{c}$). This possibility can be ruled out for the following reasons. As the Kondo effect is an isotropic effect, the N-MR should be independent of the direction of H. In fact the N-MR can be observed only for H parallel to the c-axis. The N-MR should appear in stage-2 $MoCl_5$ GIC because of relatively strong exchange interaction between spins of carriers in the bounding G layers and Mo^{5+} spins with $S = 1/2$ in the nearest neighbour I layer. In fact, the sign of cL-MR ($\boldsymbol{H} \parallel \boldsymbol{c}$) of stage 2 is positive over the whole T and H ranges examined.

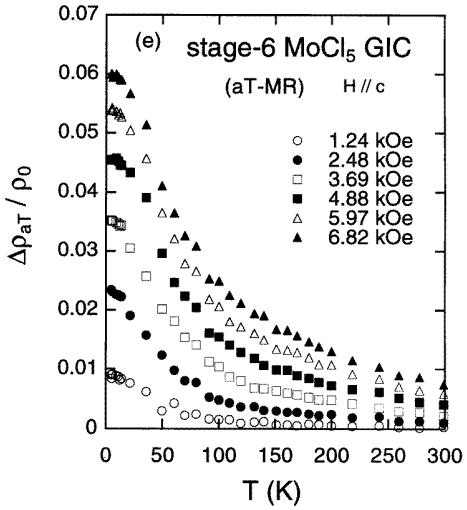

Figure 5. (Continued)

4.2.2. a-axis transverse magnetoresistance. We have measured the a-axis resistivity of stage-2 to 6 $MoCl_5$ GICs in the presence of H along the c-axis, denoted as the a-axis transverse magnetoresistance $\Delta\rho_{aT}/\rho_0$ (aT-MR ($\boldsymbol{H} \parallel \boldsymbol{c}$)). In the 2D model described in section 2, the a-axis resistivity is dominated by the in-plane resistivity of bounding G layers. When the 2D WLE occurs in the interior G layers, no N-MR contribution is predicted to be observed in aT-MR ($\boldsymbol{H} \parallel \boldsymbol{c}$). The magnetoresistance aT-MR ($\boldsymbol{H} \parallel \boldsymbol{c}$) of stage-2 to 6 $MoCl_5$ GICs is expected to be similar to that of pristine graphite. It is expected that $\Delta\rho_{aT}/\rho_0$ is positive and equal to $(\omega_c\tau_b)^2$ where $\omega_c(= eH/m_bc)$ is the cyclotron angular frequency.

Figure 4 shows the H dependence of $\Delta\rho_{aT}/\rho_0$ (aT-MR ($\boldsymbol{H} \parallel \boldsymbol{c}$)) at $T = 4.2$ K for stage-2 to 6 $MoCl_5$ GICs. Though absolute values of $\Delta\rho_{aT}/\rho_0$ for all stages are nearly the same as those of cL-MR ($\boldsymbol{H} \parallel \boldsymbol{c}$), their sign is positive over whole the H range examined, exhibiting a positive magnetoresistance (P-MR). For stage 2, the value of $\Delta\rho_{aT}/\rho_0$ increases with increasing H and is nearly proportional to H at $H \geqslant 2$ kOe. For stage 3 and 4, the slope of $\Delta\rho_{aT}/\rho_0$ against H near $H = 0$ is nearly equal to zero. For stage 5 and 6, $\Delta\rho_{aT}/\rho_0$ again increases drastically in low H. We also note that the magnitude of $\Delta\rho_{aT}/\rho_0$ at $T = 4.2$ K and $H = 6.82$ kOe is strongly dependent on the stage number: it dramatically decreases with increasing stage number from stage 2 to 4, having a minimum at stage 4, and increases with further increasing stage number. The value of $\Delta\rho_{aT}/\rho_0$ for stage 6 is almost the same as that for stage 2.

Figure 5(a)–(e) show the T dependence of $\Delta\rho_{aT}/\rho_0$ (aT-MR ($\boldsymbol{H} \parallel \boldsymbol{c}$)) for stage-2 to 6 $MoCl_5$ GICs for various H. The sign of $\Delta\rho_{aT}/\rho_0$ is positive over the whole T and H ranges examined, indicating that the P-MR contribution from the bounding G layers with high in-plane conductivity $\sigma_a(\mathrm{G}_b)$ is dominant. For stage 3 and 4, the T dependence of $\Delta\rho_{aT}/\rho_0$ exhibits a peak around 15 K, indicating the existence of a small N-MR contribution from the interior G layers with low in-plane conductivity $\sigma_a(\mathrm{G}_i)$. For stages 2 and 6 no appreciable N-MR component is observed at low T.

These results suggest that the 2D WLE does not occur in the bounding G layers for all stages. The value of P-MR for stage 3 and 4 is much smaller than that for the other stages at low H. This may be closely related to the occurrence of N-MR in the

longitudinal magnetoresistance cL-MR ($\boldsymbol{H} \parallel \boldsymbol{c}$) for stage 3 and 4. According to the 2D model described in section 2, for example, the c-axis magnetoresistance $\Delta\rho_c$ for stage-4 GIC with $G_bIG_bG_1G_1G_b$ as a c-axis stacking sequence is described by a sum of $\Delta\rho_c(G_bIG_b)$, $\Delta\rho_c(G_bG_1)$ and $\Delta\rho_c(G_1G_1)$. When the 2D WLE occurs in the interior G_1 layers, the sign of $\Delta\rho_c(G_1G_1)$ and $\Delta\rho_c(G_bG_1)$ may be negative and $\Delta\rho_c(G_bIG_b)$ is positive. Then the N-MR in $\Delta\rho_c$ may appear under the condition that the sum of $|\Delta\rho_c(G_1G_1)|$ and $|\Delta\rho_c(G_bG_1)|$ is larger than $\Delta\rho_c(G_bIG_b)$. Here it should be noted that $\Delta\rho_c(G_bIG_b)/\rho_0$ is roughly equal to $\Delta\rho_a/\rho_0$ because these quantities depend mainly on the in-plane relaxation rate of carriers in the bounding G layers. It is concluded from figures 4 and 5 that (i) the sign of $\Delta\rho_c(G_bIG_b)$ is positive for all stages, and that (ii) the value of $\Delta\rho_c(G_bIG_b)/\rho_0$ for stage 3 and 4 is much smaller than that for other stages at low T.

4.3. Condition for 2D weak localization effect

Logarithmic behaviour and N-MR have been found in $CuCl_2$, $CoCl_2$ and $SbCl_5$ GICs based on carbon fibres [20–23] and have been also discussed in terms of the 2D WLE. As far as we know, however, it has not been realized through these studies that the interior G layers plays a significant role for the c-axis conduction, partly because of the lack in data for c-axis resistivity of acceptor GICs with various stages. In the present work we have shown that the logarithmic behaviour of ρ_c (stage 3 and 4) and N-MR (stage 3 to 5) in $MoCl_5$ GICs can be qualitatively explained in terms of the 2D WLE occurring in the interior G layers.

Here we consider why the 2D WLE occurs only in the interior G layers, not in the bounding G layers. A magnetoresistance $\Delta\rho_c/\rho_0$ can be expressed by

$$\frac{\Delta\rho_c}{\rho_0} = -\frac{\Delta\sigma_B}{\sigma_B} - \frac{\Delta\sigma_{loc}}{\sigma_B} \tag{6}$$

where $-\Delta\sigma_B/\sigma_B$ and $-\Delta\sigma_{loc}/\sigma_B$ represent the semiclassical Boltzmann–Bloch term contributing to P-MR and a correction in terms of the 2D WLE contributing to N-MR, respectively. The quantity $[-\Delta\sigma_{loc}/\sigma_B]$ depends on three characteristic lengths [24, 25], i.e. a Landau length $L_H(=\sqrt{h_c/4eH})$, a mean free path L_0 associated with elastic scattering and diffusion length L_{in} associated with inelastic scattering.

To obtain N-MR, the condition

$$L_0 \ll L_H \ll L_{in} \tag{7}$$

should be satisfied. In the intermediate stages, the density of states of the interior G layer is small compared to that of the bounding G layers, because the Fermi level exists in the vicinity of bottom of its energy band. The diffusion length L_{in} associated with inelastic scattering becomes long enough and the condition (7) can be satisfied. In the transition between bounding G layers, on the other hand, the density of states of the bounding G layer is too large for the relation (7) to be satisfied. Hence it does not contribute to the logarithmic behaviour and N-MR.

The interior G layers play a role as a bottleneck to the c-axis conduction, since the observed resistivity is given by a series connection of contributions from each G layer. The logarithmic behaviour and N-MR of ρ_c arise from the 2D WLE occurring in the interior G layers. For the a-axis conduction, on the other hand, the observed resistivity is given by parallel connection and carrier conduction mainly occurs in the bounding G layers with a large density of states. The contribution of the interior G layers to the a-axis conduction is small.

The appearance of 2D WLE is more effective in the c-axis conduction. The 2D WLE is observed only in the intermediate stages. For stage-2 GICs every G layer is next to the

I layer and there is no interior G_i layer, and for high-stage ($n > 6$) GICs the graphite layers sandwiched by I layers may have a character of 3D band-like conduction.

5. Summary

For stage-2 to 5 $MoCl_5$ GICs ρ_a shows a metallic-like T dependence all over the T range, and exhibits no logarithmic behaviour. The sign of aT-MR ($\boldsymbol{H} \parallel \boldsymbol{c}$) is positive even at low T and at weak H for all stages. On the other hand, the T dependence of c-axis resistivity ρ_c of stage-2 to 6 $MoCl_5$ GICs changes from metallic-like to semiconductor-like with increasing stage number n, and a logarithmic behaviour and negative magnetoresistance are observed at low T for intermediate stages. Although our basic concept of c-axis conduction is a hopping process reflected by the in-plane relaxation time, an essential difference between a- and c-axis conduction processes is observed. These results can be explained as follows. The c-axis resistivity is expressed as a series connection of contributions from each G layer. For high stages a hopping process associated with an out-of-plane mode phonon leads to the change of T dependence from metallic-like to semiconductor-like. For the intermediate stages, transitions between interior G layers satisfy the condition of the 2D WLE at low T and H, forming a bottleneck to the c-axis conduction. This is the reason why a logarithmic behaviour and negative magnetoresistance are observed. On the other hand, a-axis resistivity is expressed as a parallel connection of contributions from G layers, so carriers are able to conduct, escaping the bottleneck. Thus, the contribution of the 2D WLE is not dominant even at low T and H.

Acknowledgments

The authors would like to thank A W Moore for providing them with HOPG samples, and C Lee and R Niver for their help in sample preparation of $MoCl_5$ GICs. They are grateful to C R Burr for a critical reading of this manuscript. The work at SUNY—Binghamton was supported by NSF DMR 9201656.

References

[1] Zeller C, Pendrys L A and Vogel F L 1979 *J. Mater. Soc.* **14** 2241–8
[2] Morelli D T and Uher C 1983 *Phys. Rev.* B **27** 2477–9
[3] Powers R, Ibrahim A K, Zimmerman G O and Taher M 1988 *Phys. Rev.* B **38** 680–8
[4] McRae E, Lelaurain M, Mareche J F, Furdin G, Hérold A and Saint Jean M 1988 *J. Mater. Res.* **3** 97–104
[5] Ohta Y, Kawamura K and Tsuzuku T 1986 *J. Phys. Soc. Japan* **55** 2338–42
[6] Ohta Y, Kawamura K and Tsuzuku T 1986 *J. Phys. Soc. Japan* **57** 196–204
[7] Andersson O E, Sundqvist B, McRae E, Mareche J F and Lelaurain M 1992 *J. Mater. Res.* **7** 2989–3000
[8] Sundqvist B, Andersson O E, McRae E, Lelaurain M and Mareche J F 1995 *J. Mater. Res.* **10** 436–46
[9] McRae E, Polo V, Vangelisti R and Lelaurain M 1996 *Carbon* **34** 101–7
[10] Andersson O E, Sundqvist B, Polo V, Vangelisti R, Mareche J F and McRae E 1996 *J. Phys. Chem. Solids* **57** 719–23
[11] Suzuki M, Lee C, Suzuki I S, Matsubara K and Sugihara K 1996 *Phys. Rev.* B **54** 17 128–40
[12] Suzuki M, Suzuki I S, Lee C, Niver R, Matsubara K and Sugihara K 1997 *J. Phys.: Condens. Matter* **9** 10 399–420
[13] Sugihara K 1984 *Phys. Rev.* B **29** 5872–7
[14] Shimamura S 1985 *Synth. Met* **12** 365–70
[15] Sugihara K 1988 *Phys. Rev.* B **37** 4752–9
[16] Sugihara K and Matsubara K 1998 *Mol. Cryst. Liq. Cryst.* **310** 255–60
[17] Sugihara K, Matsubara K, Suzuki I S and Suzuki M 1998 *J. Phys. Soc. Japan* **67** 4169–77
[18] Ibrahim A K, Zimmerman G O, Ibrahim I H, Tawfik S G and Abou-Aly A I 1994 *Physica* B **194–196** 1347-8
[19] Kamimura H, Nakao K, Ohno T and Inoshita T 1980 *Physica* B&C **99** 401–5
[20] Piraux L, Bayot V, Michenaud J-P, McRae E and Mareche J F 1985 *Solid State Commun.* **56** 567–9

[21] Piraux L, Bayot V, Michenaud J-P, Issi J-P, Mareche J F and McRae E 1986 *Solid State Commun.* **59** 711–15
[22] Piraux L, Bayot V, Gonze X, Michenaud J-P and Issi J-P 1987 *Phys. Rev.* B **36** 9045–51
[23] Piraux L 1990 *J. Mater. Res.* **5** 1285–98
[24] Lee P A and Ramakrishnan T V 1985 *Rev. Mod. Phys.* **57** 287–337
[25] Hikami S, Larkin A I and Nagaoka Y 1980 *Prog. Theor. Phys.* **63** 707–10